Eur. Phys. J. B **47**, 503–508 (2005)
DOI: 10.1140/epjb/e2005-00364-3

THE EUROPEAN
PHYSICAL JOURNAL B

First-principle calculations of the linear and nonlinear optical response for GaX (X = As, Sb, P)

Ali Hussain Reshak[a]

Physics Department, College of Science-Basra University, Basra-Iraq

Received 29 June 2005
Published online 17 November 2005 – © EDP Sciences, Società Italiana di Fisica, Springer-Verlag 2005

Abstract. The linear and nonlinear optical properties in non-centro-symmetric cubic semiconductor GaX (X = As, Sb, P) are studied by using the first-principle full potential linear augmented plane wave (FP-LAPW) and the linear muffin-tin orbital (LMTO) methods. We present calculations of the frequency-dependent complex dielectric function $\varepsilon(\omega)$ and it zero-frequency limit $\varepsilon_1(0)$. A simple scissor operator is applied to adjust the band gap from the local-density calculations to match the experimental value. Calculations are reported for the frequency-dependent complex second-order non-linear optical susceptibilities $\chi^2(\omega)$ up to 6 eV and it zero-frequency limit $\chi^2(0)$. Comparison with available experimental data shows good agreement. Our calculations show excellent agreement between the two methods.

PACS. 71.15.-m Methods of electronic structure calculations – 31.15.-p Calculations and mathematical techniques in atomic and molecular physics (excluding electron correlation calculations) – 71.15.Mb Density functional theory, local density approximation, gradient and other corrections – 42.65.-k Nonlinear optics

1 Introduction

In recent years, nonlinear optics has developed into a field of major study because of rapid advances in laser technology [1–3]. Nonlinear optical techniques have been applied to many diverse disciplines such as atomic, molecular, solid-state physics, materials science, chemical dynamics, surfaces interface sciences, biophysics, and medicine. The development of new advanced nonlinear optical materials for special applications is of crucial importance in technical areas such as optoelectronics, acoustic-optic conversions, optical signal processing, optical computing, and neuro-network implementation. There are intense efforts in experimenting, designing, fabricating, and searching for various nonlinear optical materials including semiconductors and semiconductor microstructures, ionic compounds, ferroelectric and liquid crystals, organic molecules, glasses and polymers. However there is comparatively a much smaller effort to understand the nonlinear optical process in these materials at the microscopic level. Theoretical understanding of the factors that control the figure of merit is extremely important in improving the existing electro-optic materials and in the search for new ones [3].

Even though there exist a number of calculations for the electronic band structure and optical properties using different methods [6,21,28,32,44,48]. There is a large variation in the energy gaps, suggesting that the energy band gap depends on the method of the band structure calculation. Also some of the calculated energy gaps are equal to the measured energy gaps which are not expected from calculations based on the local density approximation. We therefore thought it worthwhile to perform calculations using the full potential linear augmented plane wave (FP-LAPW) [4] and linear muffin-tin orbital (LMTO) [5] methods. In this paper, we describe detailed calculations of the band structure, density of states, linear optical properties and the second-harmonic generation (SHG) for the semiconductor GaX (X = P, As, Sb,) compound with zinc-blende structure. Our calculations will highlight the effect of replacing P by As and As by Sb on the electronic and optical properties in GaX compounds.

Our aim in this paper is to understand the origin of the high $\chi^{(2)}(\omega)$ in these materials as well as to study the trends with moving from P to As to Sb.

In Section 2 we give details of our calculations. The band structure, densities of states, the linear and nonlinear optical susceptibilities are presented and discussed in Section 3. In Section 4 we summarize our conclusions.

2 Methodology

Calculations of the non-centro-symmetric cubic semiconductor GaX (X = P, As, Sb) with zinc-blende structure are performed. The Ga atom is located at the origin and the X atom is located at (1/4 1/4 1/4). The space group is $F\bar{4}3m$. We have used the experimental lattice constant [6].

[a] e-mail: maalidph@yahoo.co.uk

The linear and nonlinear optical response has been calculated using the FP-LAPW [4] and LMTO [5] methods. Due to the cubic symmetry, we need to calculate one dielectric tensor component to completely characterize the linear optical properties. For non-centro-symmetric compounds with cubic group symmetry, only one independent nonzero element $\chi^{(2)}_{123}(\omega)$ exists out of 18 tensor element in $\chi^{(2)}_{ijk}(\omega)$.

In both the FP-LAPW and LMTO methods, self-consistency is obtained using 200 $\boldsymbol{k}$-points in the irreducible Brillouin zone (IBZ). The linear optical properties are calculated using 500 $\boldsymbol{k}$-points and the nonlinear optical properties using 1300 $\boldsymbol{k}$-points in the IBZ to obtain converged results.

3 Results and discussion

3.1 Band structure and density of states

The band structure and total density of states (TDOS) for GaX compounds are shown in Figure 1. The band structure and TDOS can be divided into three main groups/structures. From the partial DOS (not shown) we are able to identify the angular momentum character of the various structures. The lowest energy group has mainly X-s states. The second group between –7 eV to E_F is composed of Ga-d and X-p states. The last group from 1.45 for Gap, 0.4 eV for GaAs, and 0.2 eV for GaSb and above has contributions from X-p and Ga-spd states. From the partial DOS, we note a strong hybridization between Ga-d and X-p states. For all investigated compounds the valence band maximum (VBM) located at Γ. In GaP compound the conduction band minimum (CBM) is located at X resulting in indirect energy gap of about 1.45 eV. While in GaAs and GaSb compounds the CBM located at Γ resulting in a direct energy gap of about 0.4 and 0.2 eV respectively. The location of the VBM and CBM is agreed with experiment [6,29,30,41,44] and previous theoretical work [6,21,28,32–34]. The trends in the band structures (as we move from P to As to Sb) can be summarized as follows: The first group in GaAs is shifted towards lower energies by around 0.5 eV in comparison with GaP, while in GaSb it is shifted towards higher energies by around 1 eV. The bandwidth of the second group is increased. This group is shifted towards lower energies by around 0.5 eV. The bandwidth of the conduction band increases slightly by around 0.5 eV towards Fermi energy (E_F) on going from P to As to Sb causing to reduce the energy gap near Γ. In Table 1 we list the values of the energy gaps calculated by LDA along with the experimental values [6,29,30,41,44] and previous theoretical work [6,21,28,32–34]. We note that the reduction in the energy gap in agreement with the experimental data. GaAs and GaSb exhibit an overall reduction of the gap over the entire Brillouin zone. This difference in the energy gap behavior can be explained by the fact that the conduction band minimum at Γ has strong cation-s character whereas other states in the conduction band are more heavily mixed with other atomic orbitals such as anion-p states. The overall reduction in gap by substituting P by As and As by P is consistent with an overall weakening of the bonds, and, therefore, with a smaller bonding antibonding splitting.

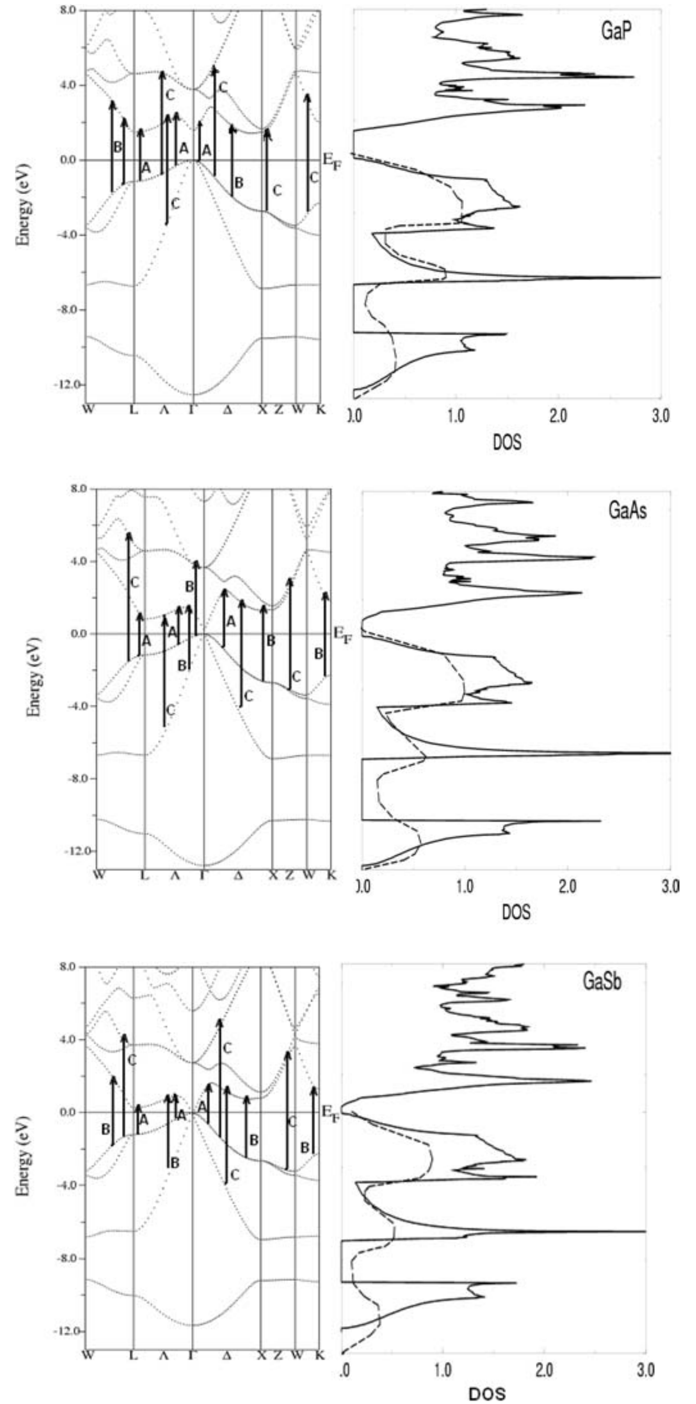

Fig. 1. Band structure and total density of states in (states/eV unit cell) compared with the X-ray photoemission spectroscopy [47]. The arrows indicate the optical transitions.

We have compared our calculated DOS with the result of X-ray photoemission spectroscopy [47]. In general, the

Table 1. attice parameters, energy gaps, and $\varepsilon_1(0)$.

	GaP	GaAs	GaSb
a (Å)	5.451[a]	5.654[a]	6.095[a]
E^{Theory}(eV)	1.22[a],2.88[g,w],2.8[j], 2.26[p], 2.28[q],2.5[e], 1.6[u], 2.05[x], **1.45**[*]	1.04[a],1.41[g,p],1.54[j],1.52[k], 1.48[q], 1.5[r], 1.527[s], 1.25[e],1.44[t], 0.2[v], 1.51[w], 1.21[x],**0.4**[*]	1.4[m],0.8[a], 0.72[g], 0.7[n], 0.661[p], 0.8[q], 0.86[w], **0.2**[*]
$E^{Exp.}$(eV)	2.38[a], 2.77[x], 2.88[h], 2.89[u]	1.52[a,x], 1.42[i]	0.8[a], 0.72[i]
$\varepsilon_1(0)$	**9.0**[*], 9.0[e], 8.8[d], 9.29[a]	**9.1**[*], 10.9[e], 11.0[d],11.21[a]	**13.0**[*], 11.42[a]
$\varepsilon_1(0)$exp	11.0[b], 9.1[f]	14.0[b], 10.9[c]	20.0[b], 14.4[c]

[a]Reference [6] [b]Reference [7] [c]Reference [14] [d]Reference [16] [e]Reference [15] [f]Reference [17] [g]Reference [28] [h]References [30,31] [i]Reference [29] [j]Reference [32] [k]Reference [33] [m]References [34,35] [n]References [34,36] [p]Reference [37] [q]Reference [38] [r]Reference [39] [s]Reference [40] [t]Reference [21] [u]Reference [41] [v]Reference [42] [w]Reference [43] [x]Reference [44] [*] **This work**.

X-ray photoemission spectroscopy (XPS) measurements are in good accord with respect to peak positioning.

3.2 Linear optical response

In the calculation of the optical response we have used the standard expression for $\varepsilon_2^{ab}(\omega)$ [3].

$$\varepsilon_2^{ab}(\omega) = \frac{e^2}{\hbar\pi}\sum_{nm}\int d\vec{k} f_{nm}\frac{v_{nm}^a\left(\vec{k}\right)v_{mn}^b\left(\vec{k}\right)}{\omega_{mn}^2}\delta\left(\omega-\omega_{mn}\left(\vec{k}\right)\right).$$

Figure 2 shows the calculated imaginary part of the frequency-dependent dielectric function along with the experimental data [7]. Broadening is taken to be 0.2 eV. Our optical properties are scissors corrected [15] by 0.1014, 0.0823 and 0.0441 Ry for GaP, GaAs, and GaSb respectively. This value is the difference between the calculated and measured energy gap. Our calculated $\varepsilon_2(\omega)$ show better agreement with the experimental data [7] than the previous calculations [15], in the mater of peak positions and structure. All the structures in $\varepsilon_2(\omega)$ are shifted towards the lower energies with reduces in the peak heights when P is replaced by As and As by Sb, in agreement with the experimental data [7]. This is attributed to the reduction in the band gaps. It would be worthwhile to attempt to identify the transitions that are responsible for the structures in $\varepsilon_2(\omega)$ using our calculated band structure. Figure 1, show the transitions which are responsible for the structures in $\varepsilon_2(\omega)$. For simplicity we labeled the transitions in Figure 1, as A, B, and C. The transitions (A) are responsible for the structures of $\varepsilon_2(\omega)$ in the energy range between 1.0 eV and 3.5 eV for GaP, 1.0 and 3.0 eV for GaAs, and 0.0 and 2.5 eV for GaSb. The transitions (B) are responsible for the structures of $\varepsilon_2(\omega)$ in the energy range 3.5 and 4.5 eV for GaP, 3.0 and 4.5 eV for GaAs, and 2.5 and 4.0 eV for GaSb. The transitions (C) are responsible for the structures of $\varepsilon_2(\omega)$ between 4.5 and 6.0 eV for GaP, GaAs and GaSb. Our calculations for the imaginary part of the frequency-dependent dielectric functions show excellent agreement between the results of the two methods. We have calculated $\varepsilon_1(0)$ and compare it with the experiments (Tab. 1). We note that a smaller energy gap yields a larger $\varepsilon_1(0)$ value. This could be explained on the basis of the Penn model [27].

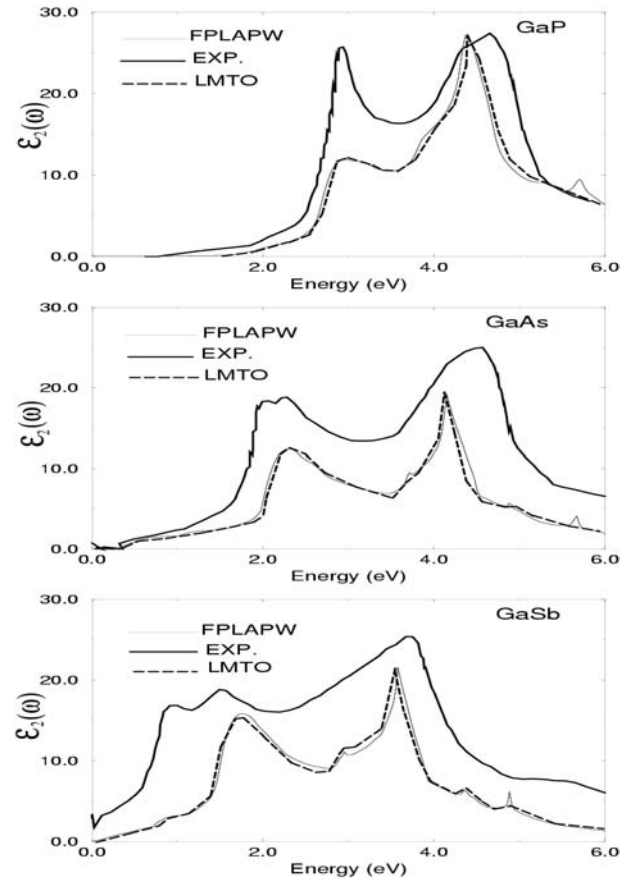

Fig. 2. Calculated $\varepsilon_2(\omega)$ using FP-LAPW and LMTO methods along with experimental data [7].

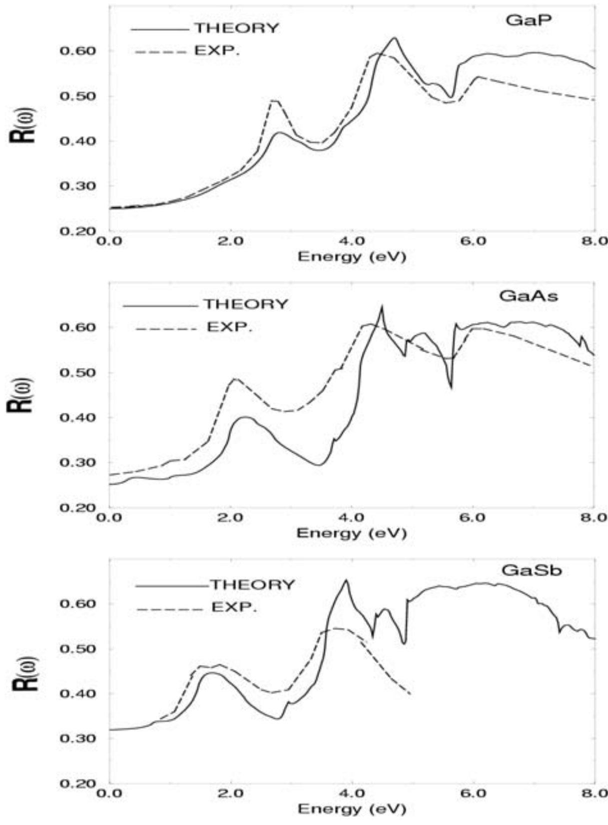

Fig. 3. Calculated reflectivity spectra for GaX compounds obtained by FP-LAPW method, compared to the experimental data: for GaP and GaAs from reference [45] and for GaSb from reference [46].

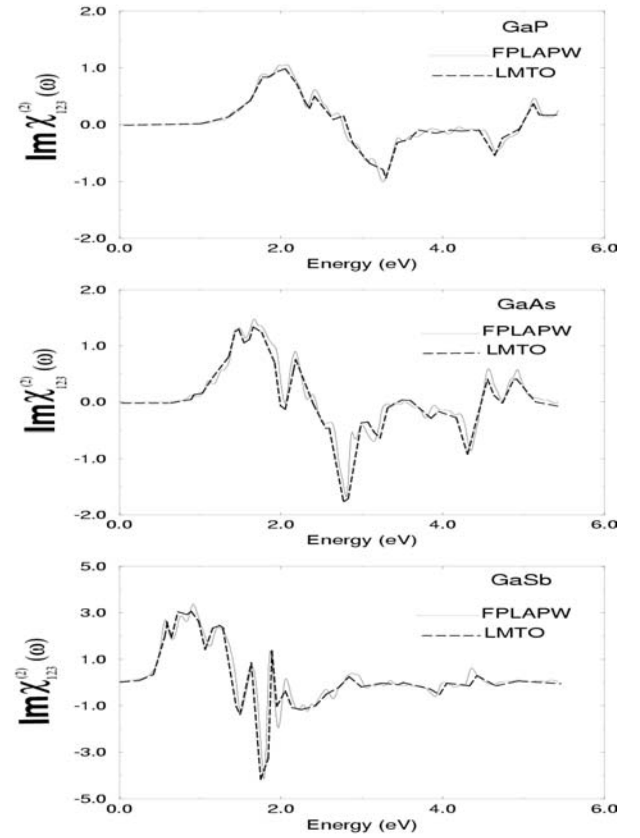

Fig. 4. Calculated $\mathrm{Im}\chi^{123}(\omega)$ in units of 1×10^{-7} esu, using FPLAPW (dark curve) and LMTO (dashed curve).

In order to make a more detailed comparison with the experimental data, we have calculated the frequency dependent reflectivity $R(\omega)$. This comparison is shown in Figure 3. It is immediately apparent that the gross features are very similar. This is due to the fact that the band structures for these compounds are indeed quite similar. We notice a strong reflectivity maximum between 1–3 eV arises from inter-band transitions. A strong reflectivity minimum at energies ranging from about 3–4 eV indicating a collective plasma resonance. The depth of the plasma minimum is determined by the imaginary part of the dielectric function at the plasma resonance and is representative of the degree of overlap between the inter-band absorption regions. The reflectivity structures shifts towards lower energies with reduction the height as we move from P to As to Sb. Comparison is made with the experimental data of Phillipp and Ehrenreich [45] for GaP and GaAs compounds and Vishnubhatla and Woolley [46] for GaSb compound. We find good agreement.

3.3 Non-linear response

The expression for the second order response $\chi^{abc}(\omega)$ can be generally written as the sum of three physically different contributions in the form [3]:

$$\chi^{abc}(-2\omega;\omega,\omega) = \chi^{abc}_{II}(-2\omega;\omega,\omega) + \eta^{abc}_{II}(-2\omega;\omega,\omega) + \frac{1}{2\omega}\sigma^{abc}_{II}(-2\omega;\omega,\omega).$$

The calculated imaginary part of the SHG susceptibility $\chi^{123}(\omega)$ obtained using the FP-LAPW and LMTO methods are shown in Figure 4. Although this part of the response function cannot be directly compared with experiment, it can be more meaningfully related to the band structure. It is well known that nonlinear optical properties are more sensitive to small changes in the band structure than the linear optical properties. That is attributed to the fact that the second harmonic response $\chi^{(2)}_{ijk}(\omega)^3$ contains 2ω resonance along with the usual ω resonance (linear response). Both the ω and 2ω resonances can be further separated into inter-band and intra-band contributions.

The structure in $\chi^{(2)}_{123}(\omega)$ can be understood from the structures in $\varepsilon_2(\omega)$. The structure between 1–4 eV is associated with interference between a ω resonance and 2ω resonances, while the structure between 4.0 and 5.5 eV is due mainly to ω resonance.

In Figure 5 we show the 2ω inter-band and intra-band contributions for GaX compounds. We note the opposite signs of the two contributions throughout the frequency range. Both the contributions increase on moving from P

Table 2. Experimental, calculated intra-band and inter-band for $\chi^{123}(0)$. $\chi^{123}(0)$ is expressed in units of 1×10^{-8} esu.

	GaP	GaAs	GaSb
$\chi^{123}(0)$ exp.	74[a], 52[f], 20[a]	162[a],90[f] 34[a]	300[f], 115[a]
$\chi^{123}(0)$total	50.3[e], 75[b], 32.2[c],43.6[d] 38[h], 24[g], **18***	96.5[e], 172[b], 60[c], 104.3[d], 96[h],38[g], **32***	70[g], 230[h], 152.9[c], 70[g], 104[i], **112***
$\chi^{123}(0)$inter	**–20***	**–30***	**–73***
$\chi^{123}(0)$intra	**38***	**62***	**185***

[a]Reference [19] [b]Reference [16] [c]Reference [6] [d]Reference [18] [e]Reference [15] [f]Reference [20] [g]Reference [12] [h]Reference [21] [i]Reference [22] ***This work**.

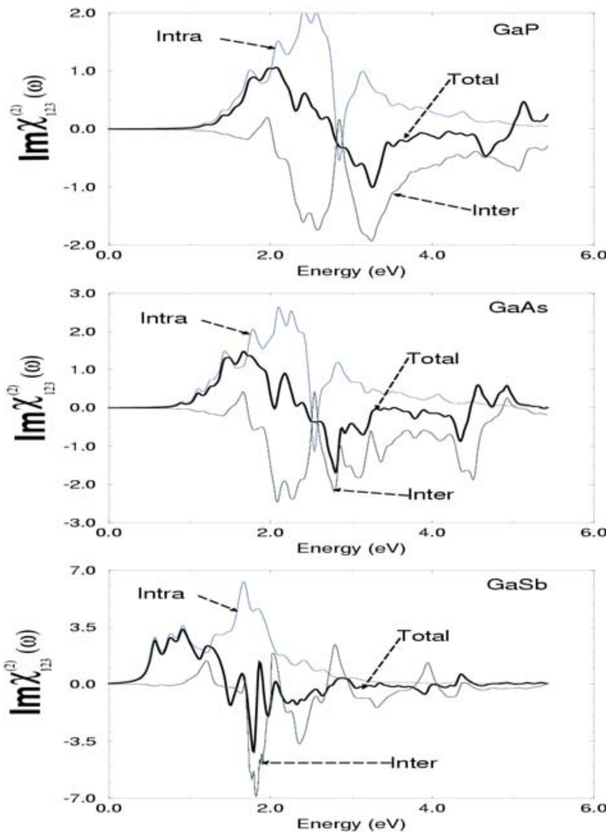

Fig. 5. Calculated $\mathrm{Im}\chi^{(2)}_{123}(\omega)$ along with the intra (2ω) and inter (2ω)-band contributions, in units of 1×10^{-7} esu , for GaX compounds.

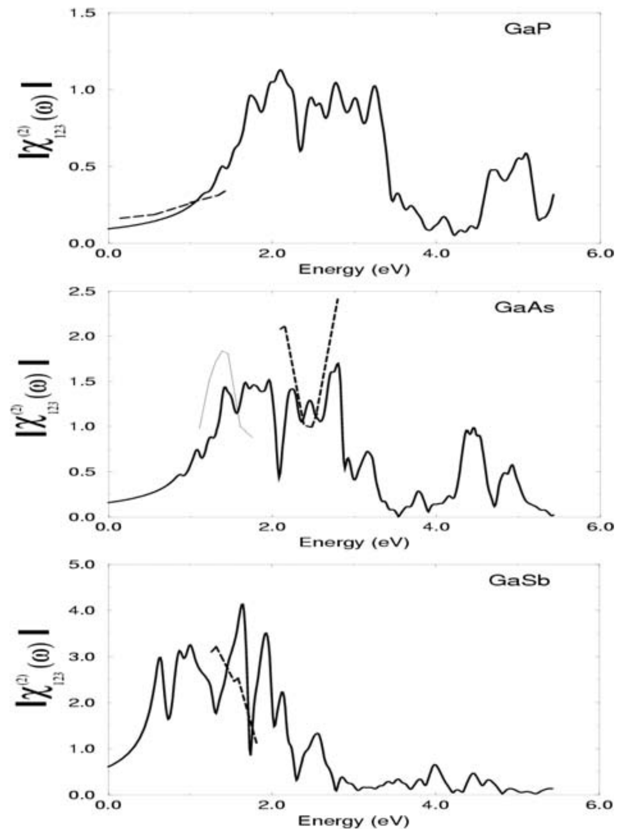

Fig. 6. Calculated $|\chi^{123}(\omega)|$ units of 1×10^{-7} esu, along with the experimental datafor: GaP from reference [23], for GaAs from reference [24] (light line) and reference [25] (dashed line), and for GaSb from reference [26].

to As to Sb. This could be attributed to the decrease in the energy gaps on moving from P to As to Sb.

Figure 6 shows our result of the $|\chi^{123}(\omega)|$ along with the experimental data [23–26]. The $|\chi^{123}(\omega)|$ is calculated from the $\mathrm{Im}\chi^{123}(\omega)$ and the $\mathrm{Re}\chi^{123}(\omega)$.

In Table 2 we present the values of $\chi^{(2)}_{123}(0)$. These values clearly increase on going from P to As to Sb in agreement with experiment and theoretical calculations. We notice that the smaller band gap compounds gives higher values of $\chi^{(2)}_{123}(0)$ in agreement with the experiment [19,20] and theory [6,12,15,16,18,21,22]. The lack of experimental data, as well as its contradictory nature, prevents any conclusive comparison with experiment over a large energy range. There is excellent agreement between the two methods of calculations.

4 Conclusions

We have performed calculations for band structure, DOS, linear and second-order optical response for GaX (X = P, As, Sb) compounds, based on FP-LAPW and LMTO

methods. Our result for band structure and DOS show that these compounds are semiconductors with energy gaps of 1.45, 0.4, 0.2 eV. We note that the energy gap reduces when P replaced by As and As by Sb in agreement with the experimental data and pervious theoretical calculations. Our calculated DOS shows good agreement with XPS data. Our $\varepsilon_2(\omega)$ and $R(\omega)$ shows better agreement with experiment data than the previous calculations. We find that the values of $\varepsilon_1(0)$ increases with decreasing energy gap, in agreement with the Penn model.

Our calculations of the SHG susceptibility show that the intra-band and inter-band contributions are significantly increased when P is replaced by As and As by Sb. All the structures in $\chi^{(2)}_{123}(\omega)$ are shifted towards lower energies when moving from P to As to Sb. Our calculations show that the smaller band gap materials have higher $\chi^{(2)}_{123}(0)$ values. Since $\chi^{(2)}_{123}(0)$ is roughly inversely correlated to the band gap, one might think that this would lead to a possible route to further enhancement of $\mathrm{Im}\chi^{(2)}_{123}(\omega)$. The enhancement of the SHG when one substitutes P by As and As by Sb is considerable. We have calculated the $|\chi^{(2)}_{123}(\omega)|$ and compare it with the available experimental data. Our calculations show excellent agreement between the two methods.

The author would like to thank the Institute Computer Center, Physics Department and Prof. S. Auluck for providing the computational facilities. Also to thank Prof. Claudia Ambrosch-Draxl and Dr. Sangeeta Sharma, Institute of Physics, University Graz, Universitätsplatz 5, A-8010 Graz, Austria for using the WIEN nonlinear code, and Prof. Sergey N. Rashkeev (Vanderbilt University, USA) for his constant help in running his LMTO code.

References

1. *Nonlinear optical properties of materials*, edited by C.M. Bowden, J.W. Hans, special issue, J. Opt. Soc. Am. B **6** (1989)
2. *Optical Nonlinearites and Instabitities in semiconductors*, edited by Harmut Haug (Academic, New York, 1988)
3. D.F. Eaton, Science **253**, 281 (1991)
4. S. Sharma, C. Ambrosch-Draxl, Physica Scripta T **109**, 128 (2004)
5. S.N. Rashkeev, W.R.L. Lambrecht, Phys. Rev. B **63**, 165212 (2001)
6. Ming-Zhu Huang, W.Y. Ching, Phys. Rev. B **47**, 9449 (1993); Ming-Zhu Huang, W.Y. Ching, Phys. Rev. B **47**, 9464 (1993)
7. D.E. Aspnes, A.A. Studna, Phys. Rev. B **27**, 985 (1983)
8. H. Lotem, G. Koren, Y. Yacoby, Phys. Rev. B **9**, 3532 (1974)
9. As listed in W.A. Harridon, *Electronic structure and the properties of solids* (Freeman, San Francisco, 1980)
10. J.J. Wynne, N. Bloembergen, Phys. Rev. **188**, 1211 (1969)
11. M.I. Bell, Phys. Rev. B **6**, 516 (1972)
12. D.E. Aspnes, Phys. Rev. B **6**, 4648 (1972)
13. J.C. Philips, J.H. Vanm Vechten, Phys. Rev. **183**, 709 (1969)
14. E.D. Palik, in *Handbook of optical constants of solids*, edited by E.D. Palik (Academic, New York, 1985), p. 429
15. J.L.P. Hughes, J.E. Sipe, Phys. Rev. B **53**, 10751 (1996)
16. Z.H. Levine, Phys. Rev. B **49**, 4532 (1994)
17. A. Borghesi, G. Guizzetti, in *Handbook of optical constants of solids*, edited by E.D. Palik (Academic, New York, 1985), p. 445
18. E. Ghahramani, D.J. Moss, J.E. Sipe, Phys. Rev. B. **43**, 9700 (1991)
19. B.F. Levine, C.G. Bethea, Appl. Phys. Lett. **20**, 272 (1972)
20. J.J. Wynne, N. Bloembergen, Phys. Rev. **188**, 1211 (1969)
21. D.J. Moss, J.E. Sipe, H.M. van Driel, Phys. Rev. B **36**, 9708 (1987)
22. B.F. Levine, Phys. Rev. B **7**, 2600 (1973)
23. M.M. Choy, R.L. Byer, Phys. Rev. B **14**, 1693 (1976)
24. R.K. Chang, J. Ducuing, N. Bloembergen, Phys. Rev. Lett. **15**, 415 (1965)
25. D. Bethune, A.J. Schmidt, Y.R. Shen, Phys. Rev. B **11**, 3867 (1975)
26. H. Lotem, G. Koren, Y. Yacoby, Phys. Rev. B **9**, 3532 (1974)
27. D.R. Penn, Phys. Rev. **128**, 2093 (1962)
28. M. Rabah, Y. Al-Douri, M. Sehil, D. Rached, Materials Chem. Phys. **80**, 34 (2003)
29. S. Adachi, J. Appl. Phys. **53**, 8775 (1982); S. Adachi, J. Appl. Phys. **61**, 4899 (1987)
30. A.C. Cartar, P.J. Dean, M.S. Skolnick, R.A. Stadling, J. Phys. C **10**, 5111 (1977)
31. D.M. Roessler, D.E. Swets, J. Appl. Phys. **49**, 804 (1978)
32. J.P. Walter, M.L. Cohen, Phys. Rev. **183**, 763 (1969)
33. C.Y. Fong, Y.R. Shen, Phy. Rev. B **12**, 2325 (1975)
34. G.W. Gobeli, F.G. Allen, J. Phys. Chem. Solids **14**, 23 (1960)
35. M.L. Cohen, J.C. Phillips, Phys. Rev. **139**, A912 (1965)
36. D.L. Greenway, M. Cardona, *Proc. international conference on the physics of semiconductors* (The Institute of Physics and Physics Society London, Exeter, 1962), p. 666
37. See *Handbook series on semiconductor parameters*, Vol. II, edited by M. Levinshtein, S. Rumyantsev, M. Shur (World Scientific, 1998)
38. Jose Maria Roman, *17th photovoltaic European conference* (2001)
39. J.R. Chelikowsky, M.L. Cohen, Phys. Rev. Lett. **32**, 674 (1974)
40. K. Kim, P.R.C. Kent, A. Zunger, Phys. Rev. B **66**, 045208 (2002)
41. S. Limpijumnong, W.R.L. Lambrecht, B. Segall, Phys. Rev. B **60**, 8087 (1999)
42. S.N. Rashkeev, W.R.L. Lambrecht, B. Segall, Phys. Rev. B **57**, 3905 (1998)
43. J.R. Chelikowsky, M.L. Cohen, Phys. Rev. B **14**, 556 (1976)
44. C.S. Wang, B.M. Klein, Phys. Rev. B **24**, 3393 (1981)
45. H.R. Philipp, H. Ehrenreich, Phys. Rev. **129**, 1550 (1963)
46. S.S. Vishnubhatla, J.C. Woolley, Can. J. Phys. **46**, 1769 (1968)
47. L. Ley, R.A. Pollak, F.R. McFeely, S.P. Kowalcyzk, D.A. Shirley, Phys. Rev. B **9**, 600 (1974)
48. G. Onida, L. Reining, A. Rubio, Rev. Mod. Phys. **74**, 601 (2002)